Inward Energy Transport in Tokamak Plasmas

T. C. Luce, C. C. Petty, and J. C. M. de Haas[(a)]
General Atomics, P.O. Box 85608, San Diego, California 92186-9784
(Received 30 August 1991)

Peaked electron temperature profiles are observed in the DIII-D tokamak during electron cyclotron heating despite the fact that > 75% of the input power is deposited significantly off axis. Power balance analysis indicates a net inward flow of energy for electrons. An inward energy flow is not compatible with diffusive or critical gradient models. A time-dependent perturbation technique is employed to estimate the conductive loss and the nondiffusive part of the energy transport. The nondiffusive component of the transport appears only at radii smaller than that of the heating location.

PACS numbers: 52.25.Dg, 52.25.Fi, 52.55.Fa

Transport of energy and particles across magnetic flux surfaces in controlled nuclear fusion experiments has been known for many years to be anomalously large [1]. Anomalous here refers to comparison with theoretical predictions based on classical collisions such as neoclassical theory, which includes the effects of the magnetic geometry [2,3]. Theoretical work to explain this anomalous transport has focused on calculations of enhanced diffusion due to turbulence generated by small-scale instabilities [1,4,5]. It is normally assumed that time evolution of the temperature T of each species in the presence of this turbulence is still governed by an equation which has the same form as the fluid equation [6]:

$$\frac{3}{2}\frac{\partial nT}{\partial t}+\nabla\cdot\mathbf{q}=Q\,, \tag{1}$$

where $\mathbf{q}$ is the heat flux. The heat sources and sinks are combined into Q. In the diffusive model, the heat flux q is assumed to be proportional to ∇T and the proportionality constant is the thermal conductivity κ. The thermal diffusivity χ is related to κ by $\kappa=n\chi$. The diffusivity could be a function of T and ∇T, which makes the equation nonlinear, and could also be a function of n and ∇n, which couples the density and temperature evolution [7]. The work reported in this Letter suggests that the assumption that the transport of energy across the magnetic field can be described solely by a (nonlinear) diffusion equation is not valid.

The experiments reported in this Letter were performed on the DIII-D tokamak [8]. The discharges analyzed here are all single-null diverted with L-mode confinement. Typical parameters are major radius $R=1.7$ m, minor radius $a=0.62$ m, toroidal field $B_T=1.7$–2.0 T, and elongation $\kappa_{\mathrm{MHD}}=1.9$.

Electron cyclotron heating (ECH) is an excellent tool for studying energy transport. The power is deposited exclusively in electrons by direct absorption. Because the absorption process is resonant, the location of the power deposition is well known and the radial spread of the power is determined by the antenna optics and refraction of the waves in the plasma. The heating location can be easily varied by changing the location of the resonance or by illuminating a different portion of the resonance in the plasma. In the cases reported here, > 75% of the total input power (ECH+Ohmic) is deposited outside the resonance location. The predicted first-pass absorption of the ECH has a narrow deposition profile with full width at half maximum ≤ 10% of the minor radius. The DIII-D ECH system was configured for launch of the extraordinary mode from the high-magnetic-field side of the plasma at 60 GHz. The waves are absorbed at the fundamental resonance where the total magnetic field is 2.14 T. The total ECH power launched was ≤ 1.25 MW.

The traditional starting point for experimental transport studies is a radial power balance analysis. For steady state, Eq. (1) implies that the net energy input is balanced by the heat flux. The heat sources and sinks are measured or calculated, so the heat flux in the radial direction is determined by integrating once over their radial distribution. Having obtained the heat flux by integration, an effective diffusivity, χ^{PB}, can be derived by dividing by the measured $n\nabla T$. The power balance analysis presented here is performed with the transport code ONETWO [9]. The measured electron and ion temperatures, electron density, effective ion charge, and radiation profiles are input, along with the magnetic geometry determined from magnetic probe measurements. The electron-ion exchange term is assumed to be classical, and the Ohmic input power is evaluated using neoclassical resistivity and the calculated current profile. The ECH deposition is calculated with the TORAY ray tracing code [10] following thirty rays to model the antenna pattern.

The experimental electron temperature profile shown in Fig. 1 provides immediate evidence of transport not in accord with purely diffusive models. Previous work [11] has shown that for diffusive transport the temperature profile should be flat inside of the heating location if the off-axis heating is the only power input. In this case, calculations indicate that more than 80% of the input power is deposited outside of $\rho=0.5$ (ρ is the radial magnetic coordinate), yet the electron temperature profile remains peaked. The anomaly is also evident in the lack of decrease in confinement from the value obtained for central heating. The electron heat flux for $\rho\le0.5$ calculated by the power balance method is clearly negative as shown in Fig. 2. The error bars are determined by varying the experimental profiles individually by their 1σ uncertainties and recalculating the power balance. The errors are combined assuming they are uncorrelated. A dramatic rever-

 © 1991 The American Physical Society

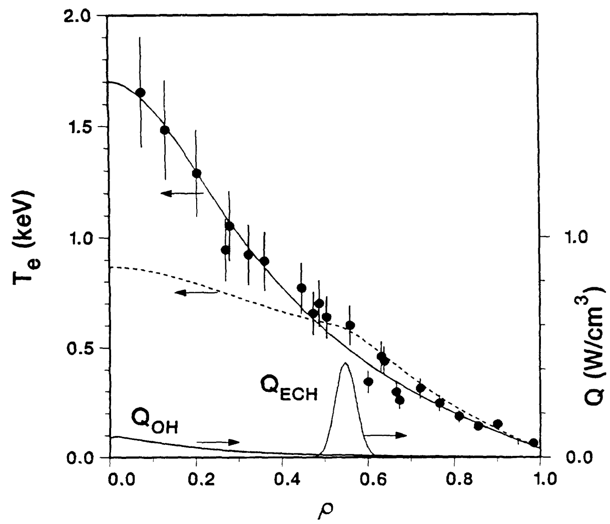

FIG. 1. Experimental electron temperature profile as a function of the radial magnetic coordinate ρ measured by electron cyclotron emission and Thomas scattering. The plasma parameters are $\bar{n}=2.2\times10^{19}$ m^{-3}, $B_T=1.7$ T, plasma current $I=600$ kA, and $P_{ECH}=1.25$ MW. The calculated power deposition profile for the ECH is also shown. The dashed curve is a simulation which is discussed in the text.

sal of the electron heat flux occurs at the ECH resonance location (ρ_{res}) as indicated in the figure. No corresponding change in the radial dependence of the ion heat flux is seen. In the region $\rho \simeq 0.3$–0.5, this power deficit is greater than the uncertainties in determining the sources and sinks. To our knowledge, this is the first measurement of radial heat flux reversal in a tokamak plasma.

Clearly, the calculated diffusivity is negative, indicating "diffusion" in the direction in which the temperature increases. There must be some outward diffusion or conduction present, at least at the magnitude predicted by neoclassical theory. Therefore, the existence of two or more energy transport mechanisms is postulated, one of which is very effective in transporting energy to regions of higher temperature. This transport mechanism is clearly not diffusive, since diffusion would act to equilibrate the temperature everywhere.

To separate the various transport mechanisms, another method must be found to estimate the magnitudes of the individual components. The power balance analysis determines the net heat flux, but cannot reveal the constituents of that flux. A time-dependent perturbation technique to determine the perturbed conductive losses has been applied to these same discharges [12]. The relaxation to the new equilibrium after a step turn-on of the ECH is observed. This relaxation occurs over many sawtooth periods. The temperature in the energy equation is written as $T_0(\rho)+T_1(\rho,t)$, where $T_0(\rho)$ is the equilibrium temperature profile during ECH. For $\partial n/\partial t=0$, the equation

$$\frac{3}{2}n\frac{\partial T_1}{\partial t}=-\nabla\cdot\mathbf{q}_1=\nabla\cdot\kappa\nabla T_1 \tag{2}$$

is solved. To obtain Eq. (2), it is assumed that the approach to equilibrium is dominated by diffusion. This does not preclude a nondiffusive term in the equilibrium energy balance. The calculated perturbed and power balance conductive fluxes can be compared by evaluating an effective χ in each case. These are illustrated in Fig. 3. Notice that the time-dependent χ is well behaved through the resonance location and agrees roughly with the power-balance χ outside the resonance location. Inclusion of effects such as a temperature-dependent χ can bring these two measurements into agreement, but this would not substantially alter our conclusions.

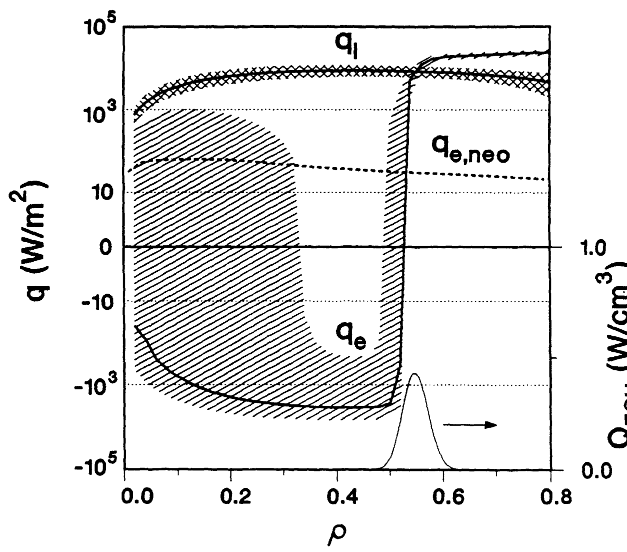

FIG. 2. Power balance calculations of the electron and ion heat fluxes and the neoclassical electron heat flux as a function of ρ for the same discharge as in Fig. 1. The ECH deposition profile is shown again for reference.

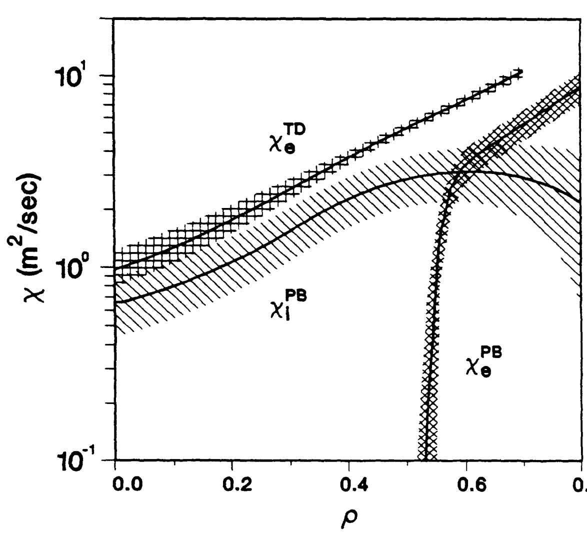

FIG. 3. Effective thermal diffusivities as a function of ρ from power balance (PB) analysis and time-dependent (TD) analysis for the same discharge as Figs. 1 and 2.

In order to estimate the magnitude and location of the nondiffusive transport and its variation with external parameters, the conductivity inferred from the time-dependent analysis is assumed to be indicative of the equilibrium conductive loss. There are systematic errors introduced by this assumption, but this method should be sufficient to indicate the relative properties of the nondiffusive transport and to give an estimate of its magnitude. The first application is to input this conductive loss in the transport code and allow the electron temperature to relax while the ion temperature, current, and radiation profiles are held fixed. The resulting electron temperature profile is shown by the dashed curve in Fig. 1. The calculated central electron temperature is almost a factor of 2 lower than the experimental value, and the profile has the expected shape for predominantly off-axis heating.

The power flowing inward at any radial location can also be calculated with the assumption that χ_e^{TD} is the equilibrium diffusivity. The power balance is solved for the "auxiliary" power density required to support the observed temperature profile against the assumed conductive loss:

$$Q_{\mathrm{aux}} = -\nabla \cdot n_e \chi_e^{\mathrm{TD}} \nabla T_e + Q_{\mathrm{rad}} + Q_{ei} - Q_{\Omega} , \qquad (3)$$

where Q_{rad} is the radiated power density, Q_{ei} is the electron-ion exchange term, and Q_{Ω} is Ohmic power density. This auxiliary power is shown in Fig. 4 along with the calculated ECH and Ohmic deposition profiles. In the event that there is no inward transport, Q_{aux} should match Q_{ECH}. The power inside $\rho = 0.6$ is sufficient to support the observed temperature profile; it is simply in the wrong place. Therefore, there must be a nondiffusive transport mechanism which very efficiently carries energy inward against temperature gradient.

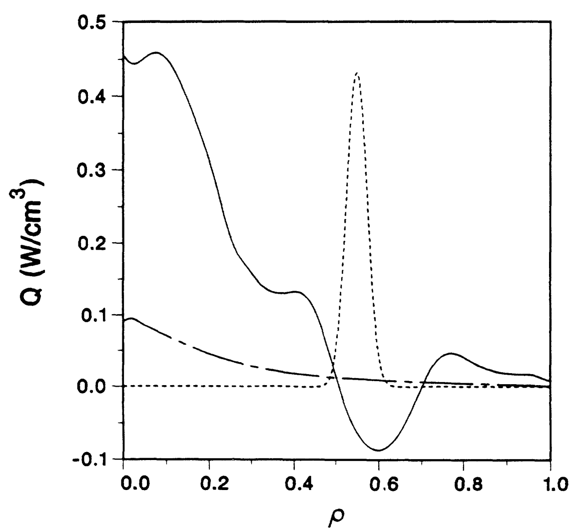

FIG. 4. Calculated power deposition profiles for Ohmic (chain-dashed), ECH (dashed), and "auxiliary" power (solid) as a function of ρ. The auxiliary power is defined in Eq. (4).

In order to understand further the nature of this nondiffusive transport, the effect of changing the location of the ECH deposition was examined. The nondiffusive flux is defined as

$$\mathbf{q}_{\mathrm{flow}} \equiv \mathbf{q}_e + n_e \chi_e^{\mathrm{TD}} \nabla T_e , \qquad (4)$$

where $\mathbf{q}_e$ is the power-balance heat flux. The radial dependence of the inward flux is shown in Fig. 5. These curves have a similar shape inside ρ_{res}, but the magnitude and location of the peak depend on the ECH deposition location. At the outermost ρ_{res}, the power flow is approximately equal to the incident power. Also shown in Fig. 5 is a case at 50% higher current with the same resonance location. It is not clear that the difference in shape is significant, but the magnitude of the peak is apparently not a function of plasma current.

There are several issues which must be discussed with regard to this analysis. If the ECH absorption were centrally peaked, no inward transport would be required to explain the peaked profile. Two observations refute this hypothesis. First, the resonance and the antennas are on the small-major-radius side of the magnetic axis. Therefore, to give the auxiliary power profile indicated in Fig. 4, the waves would have to pass undamped through the resonance where strong damping is predicted, only to be damped in a region with no known damping mechanism. Second, analysis of the initial rate of rise of the soft-x-ray signals for these discharges, as well as heat-pulse phase-lag measurements during ECH modulation experiments,

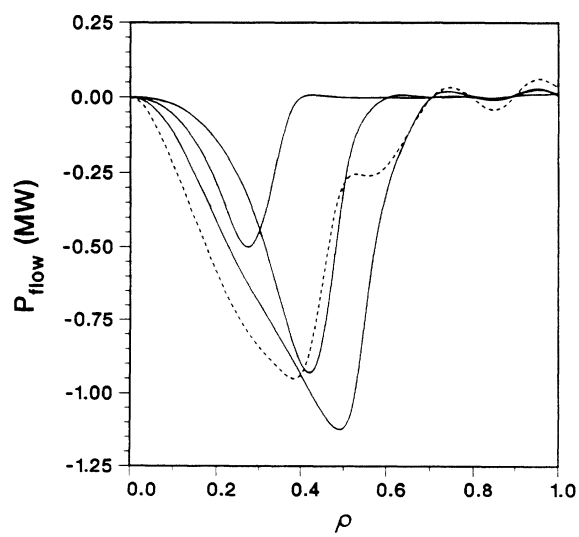

FIG. 5. Comparison of the inferred inward power flow as a function of ρ for discharges with different ρ_{res} and plasma current. The solid curves are data from a resonance position scan at constant current (600 kA). The heating location is approximately equal to the location of the peak. The dashed curve is the inward power flow for the same heating location as the middle solid curve, but at 50% higher plasma current (900 kA). The sawtooth inversion radius $\rho_{\mathrm{inv}} = 0.1-0.15$ for the 600-kA discharges and $\rho_{\mathrm{inv}} = 0.2$ for the 900-kA discharges.

indicates that energy is deposited at the location predicted by the ray tracing code. No response is observed in the center at the onset of the ECH pulse. Therefore, it is highly unlikely the observed profiles are due to direct central absorption of the electron cyclotron waves.

Another issue is the magnitude of the electron-ion coupling. The measurement errors are included in Fig. 1, but the electron-ion coupling is assumed to be classical. Enhanced coupling only accentuates the new inward flow. If the coupling is altered to reduce χ_e and χ_i to neoclassical values, the energy flow from electron-ion coupling is still in the usual direction, but is anomalously small. This implies that either the transport or the coupling must be anomalously small to explain these profiles. While it is difficult to conceive an inward transport mechanism which explains these data, it would appear to be much more difficult to explain anomalously low electron-ion coupling.

Sawtooth oscillations persist in all of these discharges despite the large drop in direct central heating. The ratio of the heating location radius to the sawtooth inversion radius varies from 2.3 to 4.1 for the discharges shown in Fig. 5. This would seem to eliminate the sawtooth as a potential cause of the inward transport.

At present, there is no theoretical explanation of the observations presented in this Letter. The data reported here place severe constraints on possible theoretical explanations. Net inward transport of energy cannot be explained by purely diffusive models even with χ as a function of T_e or ∇T_e. Models with critical temperature gradients are also excluded because these models still have neoclassical conduction as a minimum outward transport. Calculations of drift-wave transport including density gradient driven heat flux can give net inward flow of the electron energy [13], but a theory of this type which depends only on local variables cannot explain the sensitivity of the flux reversal to the heating location rather than the local fluid variables. Either there is a nonlocal transport mechanism at work in these plasmas or the appropriate local variables have not been identified.

This work is supported by the U.S. Department of Energy under Contract No. DE-AC03-89ER51114. It is a pleasure to acknowledge R. Stockdale for the use of the TRANS analysis code and useful discussions with R. Stockdale, R. Waltz, and K. Burrell. The efforts of R. Harvey, K. Matsuda, and H. St. John on ONETWO and TORAY, and of J. Lohr and R. Groebner on temperature profile analysis, and the support of R. Prater for these experiments are deeply appreciated.

[a]Permanent address: Lawrence Livermore National Laboratory, Livermore, California 94550.

[1] B. B. Kadomtsev and O. P. Pogutse, Nucl. Fusion **11**, 67 (1971).

[2] F. L. Hinton and R. D. Hazeltine, Rev. Mod. Phys. **48**, 239 (1976).

[3] S. P. Hirshman and D. J. Sigmar, Nucl. Fusion **21**, 1079 (1981).

[4] W. M. Tang, Nucl. Fusion **18**, 1089 (1978).

[5] P. C. Liewer, Nucl. Fusion **25**, 543 (1985).

[6] S. I. Braginskii, in *Reviews of Plasma Physics* (Consultants Bureau, New York, 1965), Vol. 1, p. 205.

[7] J. C. M. de Haas *et al.*, Nucl. Fusion (to be published).

[8] J. L. Luxon and L. G. Davis, Fusion Technol. **8**, 441 (1985).

[9] W. W. Pfeiffer *et al.*, General Atomics Report No. GA-A16178, 1980 (unpublished).

[10] K. Matsuda, IEEE Trans. Plasma Sci. **17**, 6 (1989); A. H. Kritz *et al.*, in *Proceedings of the Third Joint Varenna-Grenoble International Symposium on Heating in Toroidal Plasmas, Grenoble, France* (Euratom Report No. EUR70070 EN, 1982), Vol. II, p. 707.

[11] J. D. Callen *et al.*, Nucl. Fusion **27**, 1857 (1987).

[12] R. E. Stockdale, K. H. Burrell, and W. M. Tang, Bull. Am. Phys. Soc. **33**, 1977 (1988).

[13] R. E. Waltz and R. R. Dominguez, Phys. Fluids B **1**, 1935 (1989).